

ANALYSIS OF RESIDUUM DEMETALATION BY SIZE EXCLUSION
CHROMATOGRAPHY WITH ELEMENT SPECIFIC DETECTION

John G. Reynolds and Wilton R. Biggs

Chevron Research Company
Richmond, CA 94802

ABSTRACT

We analyzed thermally treated heavy residua by element specific size exclusion chromatography (SEC-HPLC-ICP) to elucidate the fate of the V and Ni compounds. Thermal treatment, in addition to removing metals, significantly reduces the size of the remaining metal-containing compounds.

We thermally treated the distillable and nondistillable metals separately. The distilled metals, primarily porphyrins, were completely processed out. The nonvolatile metals, which constituted most of the Ni and V, were either removed, or reduced in size.

When treating heavy residua over commercial fixed-bed hydroprocessing catalysts, the metal-containing molecules in the size range of the catalyst pore are preferentially removed. Those larger than the pore size appear to demetalate more slowly.

The results argue demetalation is a function of the ligand structure and size of the metal-containing species and not the coordination sphere around the metal center.

INTRODUCTION

High metals content is one of the inhibiting factors in the processing of heavy crudes and residua. These metals, particularly V and Ni, are deleterious to fixed bed catalysts, causing deactivation (1).

New technology has recently been developed to process feeds with high metals contents. This technology centers around metals removal by using high metals loading catalyst or guard beds (2), or separation and rejection of poor quality high metals materials (3).

Understanding the mechanism, or mechanisms, by which these metals are removed can ultimately lead to better processing methods. But we are limited by the methods of examination for metals. The inorganic compounds are at ppm levels, which lead to particularly difficult analytical problems. To circumvent this, we have developed and applied size exclusion chromatography, with inductively coupled plasma emission spectroscopy (SEC-HPLC-ICP) to examine V and Ni as a function of process conditions. This technique allows monitoring the size environment of a selected element, without the complications of other components.

EXPERIMENTAL

We obtained California atmospheric residua (AR) No. 1 and No. 2 by single plate distillation of the corresponding crude to a 343°C cut-point. Both AR are high in metals having over 400 ppm Ni + V.

The thermal processing was performed in a tubular flow reactor, under high hydrogen partial pressure. The fixed-bed catalytic processing was performed over commercially available metals loaded alumina catalysts at typical hydroprocessing conditions. The samples were collected from the reactors and stored cold, under nitrogen, until use. Care was taken to protect the samples from oxygen, and to analyze them as soon after processing as possible.

The processing conditions were selected based on the apparent thermal reaction threshold temperature of 410°C (see discussion below). Treatment at and above this temperature is referred to thermal processing. Three standard severities were chosen -- low, moderate, and high. Fixed-bed catalytic treatment was done below this temperature.

The fractionation of the California AR No. 1 into a porphyrin-containing distillate cut (454°C to 677°C) and a nonporphyrin-containing residuum (677°C+) was performed using a short-path distillation apparatus (DISTACT). The cut point between the two fractions was based on the earlier results on metals distribution as a function of boiling point [M. M. Boduszynski unpublished results].

We analyzed both feeds and products by SEC-HPLC-ICP. The technique and the equipment have been described in detail previously (4). The feeds and products were prepared and analyzed by the following procedure:

- 1) dilute the feed or product to a concentration of 1 to 5% by wt mobile phase of o-xylene, o-cresol, and pyridine.
- 2) elute the solution by HPLC on Ultragel 50 and 1000 nm analytical columns.
- 3) detect emission profiles of V (292.40 nm) and Ni (231.60 nm) using an ICP source.

The output, or response profile so obtained, measures the selected elemental content as a function of the elution time. Calibration with polystyrene (PS) standards (4) and model compounds (5,6), changes the response profile from a time domain to a logarithmic size domain. Because we are interested in the relative distribution, and not absolute changes, the profiles shown here are not normalized to absolute metals content.

The porphyrin/nonporphyrin separation methods are also reported elsewhere (4). UV-vis determinations were performed on alumina and capped-silica column separated fractions by techniques discussed elsewhere (4,7).

METAL STRUCTURES IN THE FEEDS

Figure 1 shows the V and Ni SEC-HPLC-ICP response profiles for California AR No. 1. The V profile exhibits the typical bimodal distribution seen for many other crudes and residua (4-6,8,9). The profiles are generally bimodal in distribution, with maxima at MW around 800 and 9000 (PS standards). The maximum at 800 has been assigned by extraction techniques to be metallopetroporphyrins (4). For the crudes examined, the metallopetroporphyrins are most of the small metal compounds, but account for only a minor amount of the

metals in the crude. 26% and 34% of the V is bound as petroporphyrin for California AR No. 1 and No. 2 respectively.

We believe the remaining metal-containing compounds are nonporphyrins. We have examined, the average first coordination sphere around the V in the nonporphyrin fraction using electron paramagnetic resonance (EPR) spectroscopy, and have found various combinations of N, S and O. For California AR No. 2, the nonporphyrin coordination sphere is N O 2S (9).

The Ni SEC-HPLC-ICP profile in Figure 1 exhibits more noise due to the lower response factor of Ni in the ICP determination in comparison with V, and the lower concentration of Ni in the feed. It also shows that there are far fewer Ni porphyrins than V porphyrins, as observed for other crudes and residua (5,6). We discuss the following results using only the V profiles. Ni profiles behaved similarly in all cases.

These results and extraction data (6) have lead to a formulation of models for metals in crude oils. We believe the metals to be of two types: 1) the porphyrins which have a narrow, but well defined molecular weight range due to homologous series substitutions (10), and 2) the nonporphyrins, which span a much broader molecular weight and size range. The nonporphyrin molecular size range could be due to small molecular weight compounds which are convoluted in a tertiary-agglomerated structure. The nonporphyrins could also have homologous series type structure.

THERMAL PROCESSING: TEMPERATURE BEHAVIOR

Figure 2 exhibits the V response profiles for California AR No. 1 thermal products. These products were generated from processing in a tubular reactor at moderate thermal severity and low thermal severity. The profiles correspond to 78% and 38% V removal, respectively.

At moderate thermal severity, the remaining metal compounds exhibit a dramatic shift to smaller molecular sizes. The larger prominent maximum is shifted from its position in the feed and appears to be vanadyl petroporphyrins. This will be discussed in a subsequent section.

At low thermal severity, the remaining metal-containing compounds exhibit similar trends, but shift much less than in the moderate thermal severity case.

These results combined with high thermal severity product profiles (not shown), indicate the extent of size reduction appears to be a function of the thermal reactor temperature.

THERMAL PROCESSING: REACTION TIME EFFECT

Figure 3 shows California AR No. 2 processed at moderate thermal severity in the tubular reactor for different reaction times. V removal was 70% in the long residence time, and 50% in the short residence time. There is little difference in the profile distribution of these products. Liquid residence time appears to have little effect on the amount of size reduction.

CATALYTIC PROCESSING

California AR No. 1 was processed downflow in a fixed-bed reactor over commercially available hydroprocessing catalysts. The V SEC-HPLC-ICP profiles of products from short residence times and long residence times are shown in Figure 4. The short residence time profile corresponds to 50% V removal. The remaining metal-containing compounds exhibit a conspicuous lack of smaller components. The porphyrin and similar size compounds are absent, while some of the larger, nonporphyrin compounds are still evident.

Fixed-bed processing at long residence time also removes the smaller metal-containing compounds. The long residence time profile corresponds to 70% V removal. The profile is very similar to that of the short residence time profile showing the longer reaction time does not appear to affect the size profile of the remaining metal-containing compounds. This is also seen in the thermal treatment results above.

Under fixed-bed processing conditions, the catalyst pore size appears important. The compounds that are in the size range of the catalyst pore are removed. This behavior has been seen in the studies on the processing of Safaniya asphaltenes (11), Arabian Light vacuum residuum (VR) asphaltenes and maltenes (12), in gel permeation chromatography (GPC) studies of Venezuelan crudes (13), and in demetalation kinetic studies of Boscan and Arabian Light residua (14).

The metal-containing compounds which do not fit in the catalyst pores require more severe processing. Longer residence times were required to remove these metals. The kinetics of metals removal over typical hydrodesulfurization catalysts have been determined in some cases to be second order (15). This has been explained as demetalation by two different first-order rate constants (16). These could be the respective demetalation rates for the metals which can fit into the catalyst pores and those which cannot.

THERMAL PROCESSING: PORPHYRINS AND NONPORPHYRINS

To determine the individual fates of the porphyrins and nonporphyrins during processing, California AR No. 1 was separated into distillable and nondistillable metal fractions by distillation, and each fraction was thermally processed. Figure 5 shows the separation by distillation. The 454°C to 677°C fraction shows only small size metal-containing compounds. The V in this fraction was determined by UV-vis spectroscopy to be 98% porphyrin, and by methanol extraction to be 90% porphyrin. The 677°C+ fraction is primarily the nonporphyrin metal compounds. Methanol extraction indicates only 2% of the V bound as porphyrin, and UV-vis spectroscopy indicates only 2% of the V bound as porphyrin in this fraction.

For thermal treatment at moderate thermal severity both fractions were diluted with appropriate vacuum gas oil components to their original metals concentration in the AR. Figure 6 shows the V SEC-HPLC-ICP profiles of the 454°C to 677°C fraction before and after processing. It is clear from the profiles that the porphyrins are completely removed (as well as the rest of the V).

Figure 7 shows the V SEC-HPLC-ICP profiles for the 677°C+ fraction before and after moderate thermal severity treatment. The remaining metal-containing compounds are shifted to the smaller

molecular size, similar to those of the moderate thermal severity processing of California AR No. 1.

Nonporphyrins have been thought of as porphyrins which have been encapsulated in an agglomerative network (17). They would not necessarily be detected as porphyrins because their spectroscopic and physical properties could be changed by this agglomeration. The size reduction seen in the thermal treatment of the 677°C+ cut produces compounds which are smaller than either the feed petroporphyrins, or porphyrin model compounds, as evidenced in Figure 7. Porphyrin extraction and UV-vis determination show less than 3% of the V is bound as petroporphyrin in this product. We feel this verifies the existence of the nonporphyrins which are not encapsulated porphyrins.

This argument would be nullified if the structure of the metal-containing compounds were sufficiently changed during processing. For example, the porphyrins could be demetalated, but instead of falling out completely, the metals could combine with other polar organic molecules and could rebind having a nonporphyrin ligand environment.

DISCUSSION

The results shown here are important in the overall picture of processing residua and heavy oils. Although little data exists on the behavior of the metal-containing compounds monitored by element specific detection, some studies have been done by other techniques.

GPC studies on the organic portion of Arabian Light VR maltenes and asphaltenes thermally processed under vis-breaking conditions showed a dramatic decrease in the average molecular size (12) upon increase of process temperature. The same results were found in the heat treatment of Safaniya VR asphaltenes (11). This agrees well with our thermal processing results for the Ni and V, where we also see size reduction which is dependent on thermal temperatures.

The effect of fixed-bed processing under catalytic conditions has been studied more thoroughly. Arabian Light treated under mild hydroprocessing conditions exhibited metals reduction corresponding to catalyst pore size (14). Similar results for the organic portion have been seen with Arabian Light VR asphaltenes (12), Morichal crude (13), and asphaltenes from Safaniya VR (11). This also agrees well with our fixed-bed processing results where the metals are distinctively affected by the pore size of the catalyst.

One of the important consequences of this study is that the porphyrins appear to be removed first in residuum demetalation. This conclusion has been reached previously. Porphyrins have been found to be preferentially removed in thermal treatment with hydrogen and/or hydrogen sulfide (18). In addition, the reaction threshold temperature for porphyrin demetalation was 400°C without, but only 200°C with a fixed-bed hydrogenative catalyst. Oxidative treatment studies of residua have also shown the same effect -- the porphyrins come out first (19,20).

Our studies support these conclusions. The results from separate processing of the porphyrins and the nonporphyrins are evidence that the porphyrins are the most labile. In addition, the removal of the metals is greatly assisted by the fixed-bed hydroprocessing catalyst, which operates at a substantially lower temperature.

However, it is important to note that these results may not be a consequence of the porphyrin or the nonporphyrin coordination sphere, but simply a consequence of the size of the compounds. In the thermal case, the porphyrins were removed because they were most of the smallest metal-containing molecules. In the fixed-bed processing, the porphyrins were removed because of the metal-catalyst pore size relationship.

Studies of feeds and products from the ABC process (21), showed the isotropic EPR parameters of the vanadyl ion exhibited little change in processing, and therefore little or no change in the first coordination sphere about the metal center (22,23). It was concluded from this that the reactivity of the vanadium is determined by the macrostructure of the residuum, and not by the nature of the coordinating metal ligands.

This is also supported by the rates of hydrodemetalation studies of extracted petroporphyrins. The facility by which hydrogenation of porphyrins (24) occurs strongly argues the rate of demetalation is not a function of the intrinsic reaction rate of the first coordination sphere around the metal ion, but diffusion through or denaturing of the polar medium around the metal-centers.

CONCLUSION

We have examined thermal processing and catalytic fixed bed processing by SEC-HPLC-ICP to determine demetalation mechanisms. Thermal processing removes Ni and V and reduces the size of the remaining metal-containing compounds. Fixed-bed processing removes metals as a function of the pore size.

By separating the porphyrins from the nonporphyrins, we have found the porphyrins process the easiest under thermal conditions. This could be a result of their intrinsic reactivity, or merely a function of size or macrostructure. It is our contention, the macrostructure is rate controlling for at least the nonporphyrins.

ACKNOWLEDGEMENTS

The authors would like to thank Sue Bezman for the fixed-bed processed samples, Mietek M. Boduszynski and Tim Attoe for the short-path fractionation of the AR into porphyrin-containing distillate and nonporphyrin-containing residuum, Rick Brown and Jim Gano for assistance with the ICP, Thomas Finger for assistance in sample work-up, and Chris Kuehler for helpful discussions.

REFERENCES

1. Tamm, P. W., Harnsberger, H. F., and Bridge, A. G. 1981. Ind. Eng. Chem. Process Des. Dev., 20:263.
2. Busch, L. E., Hettinger, W. P., Jr., and R. P. Krock. 1984. Oil and Gas J., 82(52):54-56.
3. Bunch, R. A., Kocisicin, J. J., Schroeder, H. F., and G. N. Shaw. 1979. Hydrocarbon Processing, 59(9): 136.
4. Biggs, W. R., Fetzer, J. C., Brown, R. J., and J. G. Reynolds. 1985. Liq. Fuel Tech., 3(3), XXX.

5. Fish, R. H., and Komlenic, J. J. 1984. Anal. Chem., 56:510-517.
6. Fish, R. H., Komlenic, J. J., and Wines, B. K. 1984. Anal. Chem., 56:2452-2460.
7. Sundararaman, P. 1985. Anal Chem., submitted.
8. Reynolds, J. G., Biggs, W. R., Fetzer, J. C., Gallegos, E. J., Fish, R. H., Komlenic, J. J., and Wines, B. K. 1984. Proceedings of the international symposium on crude oils and petroleum residues, Lyon, France, pg 153-157, June.
9. Reynolds, J. G., Biggs, W. R., and Fetzer, J. C. 1985. Liq. Fuel Tech., 3(3), XXX.
10. Baker, E. W. 1967. J. Amer. Chem. Soc., 88(10):2311-2315.
11. Drushel, H. V. 1976. ACS Div. of Petrol. Chem., Preprints, 21(1):146.
12. Hall, G. and Herron, S. P. 1981. ACS Adv. Chem. Ser., 195:137.
13. Sanchez, V., Murgia, E., and Lubkowitz, J. A. 1984. Fuel, 63:612.
14. Bridge, A. G., and Green, D. C. Green. 1979. ACS Div. Pet. Chem., Preprints, 24:791.
15. Oleck, S. M. and Sherry, H. S. 1977. Ind. Eng. Chem. Process Des. Dev., 16:525.
16. Agrawal, R., and Wei, J. 1984. Ind. Eng. Chem. Process Des. Dev., 23:505-514.
17. Yen, T. F. 1975. In The Role of Trace Metals in Petroleum. T. F. Yen Ed., Ann Arbor Science. Ann Arbor, MI. Chapter 1.
18. Rankel, L. A. 1981. ACS Div. of Petrol. Chem., Preprints, 26(3):689-698.
19. Gould, K. A. 1980. Fuel, 59:733-736.
20. Sugihara, J. M., Branthaver, J. F., and Wilcox, W. 1973. ACS Div. of Petrol. Chem., Preprints, 18:645-647.
21. Asaoka, S. Nakata, S., Shiroto, Y., and Takeuchi, C. 1983. Ind. Eng. Chem. Process Des. Dev. 22:242-248.
22. Dickson, F. E., Kunesch, C. J., McGinnis, E. L., and Petrakis, L. 1972. Anal. Chem., 41:576.
23. Dickson, F. E., and Petrakis, L. 1974. Anal. Chem., 44:1129.
24. Rankel, L. A., and Rollmann, L. D. 1983. Fuel, 62:44-46.

FIGURE 1
SEC-HPLC-ICP PROFILES FOR
CALIFORNIA AR NO. 1

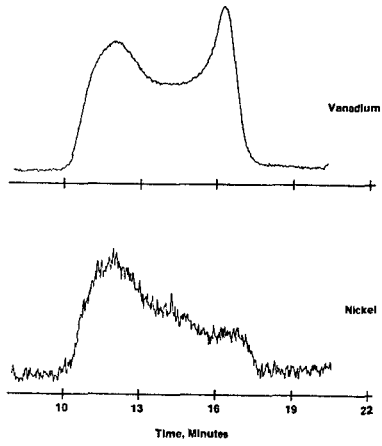


FIGURE 2
CHANGES IN VANADIUM DISTRIBUTION FROM
THERMAL TREATMENT OF CALIFORNIA AR NO. 1

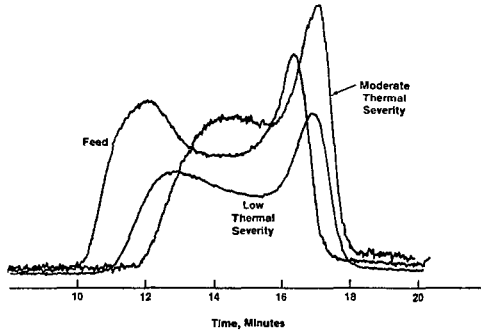


FIGURE 3
CHANGES IN VANADIUM DISTRIBUTION FROM
THERMAL PROCESSING OF CALIFORNIA AR
NO. 2 AT DIFFERENT RESIDENCE TIMES

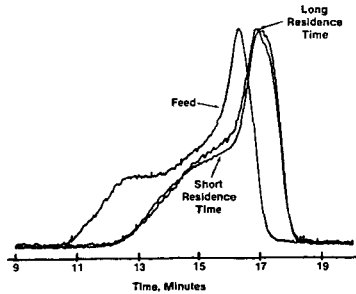


FIGURE 4
 CHANGES IN VANADIUM DISTRIBUTION FROM
 FIXED-BED TREATMENT OF CALIFORNIA AR NO. 1 AT
 DIFFERENT RESIDENCE TIMES

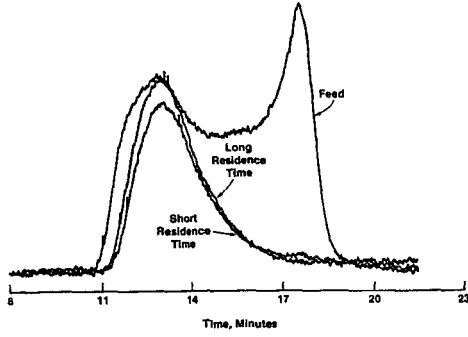


FIGURE 5
 VANADIUM SIZE PROFILES OF CALIFORNIA AR NO. 1,
 454°C to 677°C DISTILLATION CUT, 677°C+ RESIDUE

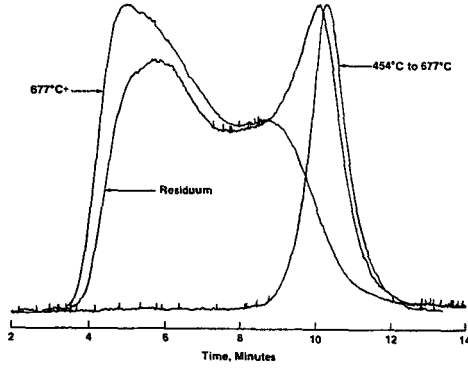


FIGURE 6
 CHANGE IN VANADIUM SIZE DISTRIBUTION OF THE
 454°C to 677°C DISTILLATION CUT OF CALIFORNIA
 AR NO. 1 UPON THERMAL TREATMENT

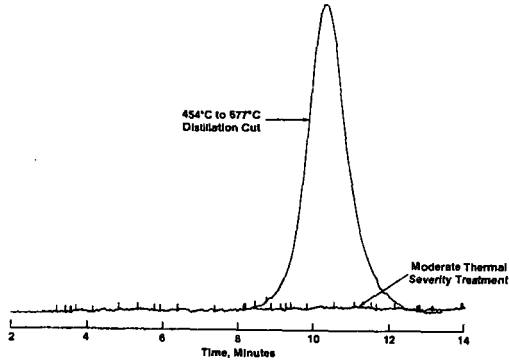
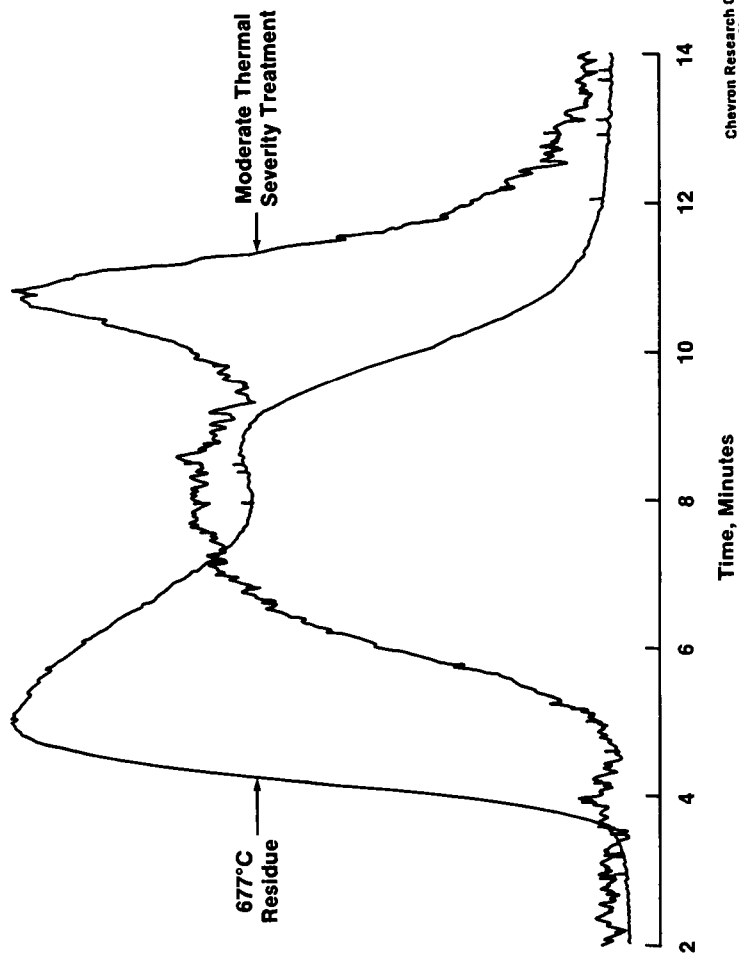


FIGURE 7

**CHANGES IN VANADIUM SIZE DISTRIBUTION OF THE
677°C+ RESIDUE OF CALIFORNIA AR NO. 1
UPON THERMAL TREATMENT**



Chevron Research Company
Richmond, California
JGR SA 851575

EFFECT OF TRACE METALS ON FCC COKE YIELD

Periaswamy Ramamoorthy
Gulf Research and Development Company
P. O. Drawer 2038
Pittsburgh Pa 15230

An experimental study is underway at the Gulf Research Center in Harmorville, Pennsylvania, aimed at defining the effects of trace metals on the regeneration of fluid cracking catalysts for resid cracking applications. As part of this study a benchscale experimental technique was developed for coking the FCC catalysts under well-mixed conditions. Coke yield was found to correlate well with the type of metal and its concentration.

When contact time was varied the coke yield obeyed the well-known Voorhies-type correlation for each metal:

$$C = AT^n$$

where C is weight percent carbon on the catalyst, T is contact time in minutes, A and n are constants. The experimental technique and results obtained for nickel, antimony, and nickel passivated with antimony are discussed in this paper.

The apparatus used for coking consisted of a shaker bomb with a dipleg as shown in Figure 1. The shaker bomb containing a known weight of catalyst was placed in a fluidised sandbath and heated to a typical temperature of 930 F under nitrogen purge. An oil feed was added at a constant rate to the catalyst over a period of time required 1 minute. The internal catalyst temperature was measured by a thermocouple placed at the center of the dipleg. At the end of run the shaker bomb was transferred to another fluidised sandbath maintained at room temperature. The catalyst was then discharged and its carbon content determined. In addition to carbon, the coke was analysed for hydrogen, sulfur, and nitrogen.

Results obtained for nickel, antimony, and nickel passivated with antimony are discussed here. The metals were added, separately and in combined form, to a batch of an equilibrium catalyst at four concentration levels.

Catalysts containing freshly deposited nickel alone showed a steady increase in coke yield with metal content. When antimony was added to passivate nickel on catalyst a reduction in coke make of approximately 40% was obtained. Typical reduction of 50% is reported for commercial units.

Catalysts containing freshly deposited antimony alone did not affect coke yield, regardless of its concentration.

Coking runs made on aged catalysts of high metal content resulted in coke yield lower than that predicted by the correlation developed

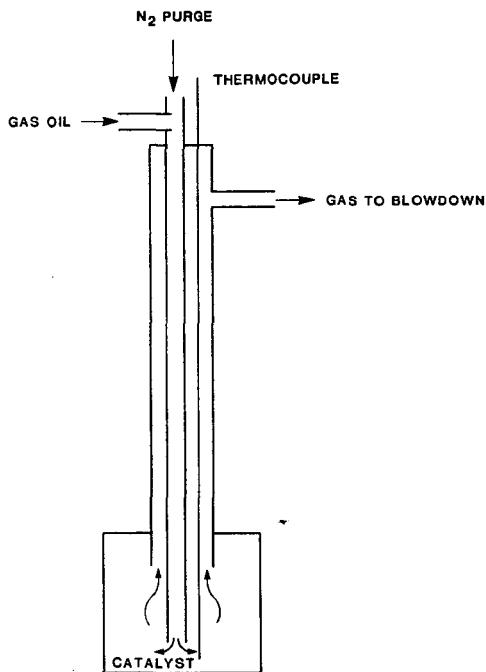
for fresh-metals catalysts.

ACKNOWLEDGEMENT

The author wishes to thank Dr. A. S. Krishna of Gulf Research and Development Company for helpful discussions during the course of this study.

REFERENCE

1. Voorhies, Jr., A., Ind. Eng. Chem., 37(4), 318 (1945)



SHAKER REACTOR FOR COKING

THE INFLUENCE OF THE PETROLEUM RESIDUA AND CATALYST TYPE ON COPROCESSING

Christine W. Curtis, Kan-Joe Tsai,
and James A. Guin

Chemical Engineering Department
Auburn University, Alabama 36849

Introduction

The goal of coprocessing heavy petroleum crudes and residua with coal is to simultaneously upgrade both materials into higher quality liquid products. Among the benefits of coprocessing is that it offers a bridge between the present petroleum-based technology and the synthetic fuels coal-based technology of the future. Coal and petroleum residua are both low value hydrocarbon resources, which through coprocessing can be transformed into higher quality and higher value synthetic fuels. The nature of the synthetic fuel produced from coprocessing would be quite different from that of conventional coal liquefaction using a coal-derived recycle stream. The highly aromatic coal-derived synthetic fuel would already be combined with ample quantities of highly paraffinic materials, making the product more similar to fuels used today. In addition, the presence of coal-derived synthetic fuel in the coprocessing product would serve as an octane booster. Another advantage of coprocessing is the elimination or minimization of the coal-derived recycle stream used in conventional coal liquefaction technology.

A number of petroleum materials have been surveyed for their ability to solvate coal and to participate in the upgrading process. (1-4) Both bituminous and subbituminous coals have been successfully used in combined processing (5,6). Using catalytic hydrotreatment with small particle size catalysts, coal conversion of greater than 80% have been achieved for both bituminous and subbituminous coals when using petroleum solvents.(5) The interaction between the petroleum solvent and the coal is complex. Synergistic interactions may exist at different concentration levels of coal and petroleum solvent. In this work the interaction between the petroleum solvent and coal at different solvent to coal ratios is examined in terms of product yield and coal conversion. The chemical composition of the petroleum solvent is substantially different from coal-derived solvents.(1) The effect of improvement in the solvent's ability to donate hydrogen through the addition of hydroaromatic compounds on the final product slate has been investigated. Because of the complexity and diversity of the coal-petroleum system, catalyst type may strongly influence one material while not being particularly effective with the other. Examination of the effect of catalyst type on the upgrading of the petroleum residuum and on coprocessing can lead to catalysts that are specifically tailored for enhancement of the coprocessing product slate. In addition, the coprocessing product may be enhanced through a combination of a first stage reaction using a mineral additive and a second stage with a commercial hydrogenation catalyst. This concept is explored in this work.

Experimental

Materials and Feedstocks

The solvents used in this study were heavy petroleum crudes and residua which were supplied by Cities Service Research and Development Company. The specific petroleum materials used were Maya toppler long resid (TLR) and West Texas vacuum short resid (VSR). A bituminous Illinois #6 coal, supplied by Wilsonville Advanced

Coal Liquefaction Research and Development Facility, was used as the coal feedstock. The elemental analyses of these feedstocks are given in Table 1. The catalysts used in these reactions were mineralogical pyrite ground to -200 mesh and powdered presulfided Shell 324 NiMo/Al₂O₃ that was obtained by grinding 1/16 inch presulfided extrudates. For the hydrogen donor addition experiments, tetralin, 1,2,3,4-tetrahydroquinoline (THQ) and 9,10-dihydrophenanthrene (DHP) were obtained from Aldrich.

Equipment

The combined processing reactions were conducted in stainless steel micro-reactors which have been described in a previous work (7). The reactor has a volume of 50 cc which was charged with a liquid/solid slurry of 9 g and a hydrogen pressure of 1250 psig at ambient temperature at 100% excess hydrogen for the combined processing reactions. A 6g charge was used for the petroleum upgrading experiments. The pressure of 1250 psig at ambient temperature corresponds to approximately 2950 psig at reaction temperature calculated by means of the ideal gas law and ignoring any solubility of the hydrogen. A recovery of greater than 97% of the original charge was obtained from the coprocessing reactions.

Experimental Procedures

A series of experiments were performed using Illinois #6 coal and West Texas VSR in which the solvent to coal ratio was varied from 10:1 to 1:4. The percentage coal present in these reactions ranged from 9.1% to 80%. For comparison, reactions were also performed in which no coal was present and in which no solvent was present. The reaction products were analyzed by a solvent extraction procedure in which the reaction products were sequentially extracted with pentane, benzene, and methylene chloride/methanol. The products obtained were defined as oil, pentane soluble; asphaltenes, pentane insoluble, benzene soluble; preasphaltenes, benzene insoluble, methylene chloride/methanol soluble; and insoluble organic matter (IOM), methylene chloride/methanol insoluble. Analyses performed on the products of the coprocessing reactions were: (1) viscosity at 60°C according to ASTM D-2171 using a Canon-Manning capillary viscometer, (2) specific gravity at 60°F according to ASTM D-70 and ASTM D-287, and (3) Conradson Carbon according to ASTM D-189.

The coprocessing reactions with the addition of hydroaromatic solvents were performed at 425°C, in a N₂ or H₂ atmosphere, for 30 minutes. The charge to the reactor was 3 grams of Illinois #6 coal and 6 grams of total solvent. The solvent was composed of 0.3 g, 1.1 g or 3.0 g of hydroaromatic compound with 5.7 g, 4.9 g or 3.0 g of Maya TLR, respectively. The pressure of H₂ charged to the reactor was 300 psig and of H₂ was 1250 psig.

Mineralogical pyrite and small particle size NiMo/Al₂O₃, ground from presulfided 1/16" extrudates were used to determine the effect of catalyst type on the upgrading of West Texas VSR and on coprocessing of Illinois #6 coal with West Texas VSR and Maya TLR. The reactions were performed at 425°C, 30 minutes, with 6 g of petroleum solvent, 3 g of coal and 1 g of catalyst.

The reaction conditions for single stage processing were 60 minutes, 425°C, 1250 psig H₂ charge, and 2 grams of catalyst. The catalysts used were pyrite, NiMo/Al₂O₃ and H₂S which was generated in situ from the reaction of carbon disulfide with hydrogen.

The two stage experiments were performed as two sequential 30 minute reactions at 425°C, 1250 psig H₂ charge, 9 grams of petroleum/coal slurry and 1 gram of catalyst in each stage. The gas weight was determined after the first stage; the reactor was then opened and the second stage catalyst was added. After repressurizing with hydrogen, a second reaction was performed. The total gases were calculated through the addition of the gases produced during each stage. The first stage mineral catalyst was not removed and was present in the second stage reactions. For the calculations of the final amount of reacted FeS₂ remaining, the FeS₂ is assumed to react completely to form FeS.

Results and Discussion

To tailor the coal-resid system for maximal yields of high quality liquid products, the influence of the petroleum solvent on the products obtained from coprocessing must be known. Addition of additives such as hydrogen donors may enhance the desired product yield. With two complex and diverse materials present, catalyst selection becomes more complex, for a particular catalyst may catalyze reactions of one of the materials much more strongly than the other. Combination of catalyst types may prove feasible to achieve the many diverse reactions needed to achieve high coal conversion and high yields of liquid product simultaneously.

The Effect of Solvent to Coal Ratio on Coprocessing

One of the advantages of coprocessing is the elimination or minimization of the coal-derived recycle stream needed in conventional coal liquefaction technology. In conventional liquefaction the solvent to coal ratio usually ranges from 1:1 to 3:1 with the ratio being dependent on the materials used and the operability and range of the mechanical equipment. In coprocessing, a limitation on the solvent to coal ratio will still exist due to physical constraints. In this study, however, we investigated a wide range of solvent to coal ratios to observe the effect of the solvent concentration on the final product distributions obtained. At low solvent to coal ratios, the mass transfer of the hydrogen to the coal may be inhibited. At high solvent to coal ratios, the coal may serve as an extender or enhancer to the petroleum material, by synergistically promoting the upgrading of the petroleum material.

The range of solvent to coal ratios examined was 10:1 to 1:4. The reactions were performed at the coprocessing conditions given in the Experimental section. In these experiments, the reactor liquid plus solid loading was kept constant so that nine (9) grams of petroleum-coal slurry was introduced each time. The amount of catalyst used in each reaction remained constant at one gram. Since both the percentage solvent and coal changed in each reaction, experimental results must be expressed independently of the amounts of petroleum solvent and coal. The hydrogen consumption and coal conversion can be used directly. The amount of material upgraded to oil can also be determined independently of the system by defining it as oil production which is the grams of oil produced (final oil-initial oil) divided by amount of the upgradable material. The upgradable material is composed of maf coal and the nonpentane soluble fraction of the solvent.

As the percentage of coal increased from 9.1% to 50%, coal conversion increased from 42.6% to 87.2% as presented in Figure 1. At increasingly higher levels of coal, the amount of coal conversion steadily decreased. When no solvent was present, a coal conversion of 33% was obtained. Hydrogen consumption, shown in Figure 2, followed the same trend, giving a maximum at 50% coal loading. The percent oil production achieved at coal percentages of 25% to 50% was constant at

~33% as shown in Figure 3. A similar value of 28% oil production was obtained at 9.1% coal loading. At higher coal loading, the percent oil production decreased rapidly, falling to ~15% at 80 and 100% coal loading.

The complexity of the coprocessing reaction system and the many reactions which occur simultaneously make it difficult to ascertain the reasons for the behavior observed as the solvent to coal ratio was varied. The interrelation-ship among coal conversion, oil production and hydrogen consumption is evident. Hydrogen consumption is directly related to the amount of coal conversion achieved and the amount of oil production observed. The behaviors of coal conversion and oil production as a function of the increased weight percentage of coal in the reactions are more difficult to explain.

Numerous factors may be influencing these behaviors and causing interactive effects. Some of the factors involved may be mass transfer effects, concentration of the coal and solvent blends, compositional effect of the blend of liquefied materials, catalyst poisoning and deactivation and solvolysis of the dissolving coal matrix by the liquid phase present. Since in coprocessing, the molecular composition varies rather dramatically from high solvent to coal ratios to low solvent to coal ratios, solvolysis of the dissolving coal matrix by the liquid present in the reactor may be an important factor in the observed behavior of coal conversion and oil production. The 50% blend of coal to petroleum solvent may provide a good coal dissolving solvent. Mass transfer of H_2 to the dissolving coal matrix is most likely better achieved when a higher proportion of solvent is present. Therefore, the higher yields of oil and of coal conversion achieved at higher solvent to coal ratios compared to the lower ratios may be due to the increased availability of hydrogen to the coal. The decline at high coal loadings may be due to mass transfer limitations on H_2 . In this system, however, it must be remembered that the coal to catalyst ratio increased as the coal loading increased; or stated in another manner, the catalyst loading remained constant as the percent coal in the reaction increased. The decline in coal conversion and oil production may be due to catalyst deactivation and rapid loss of activity in the concentrated coal matrix. As stated earlier, the exact reasons for the behavior observed can not be pinpointed. One possible rationale is that several different mechanisms are occurring and that different mechanisms are dominant at different coal concentrations.

Analyses of some of the physical properties of coprocessing reaction products have been performed and are compared to the original coprocessing solvent, West Texas VSR, and hydrotreated West Texas VSR in Table 2. Products obtained from reactions using a 10:1 solvent to coal ratio and a 2:1 solvent to coal ratio were examined. The physical properties evaluated were viscosity, degrees API gravity, specific gravity and Conradson Carbon. In the hydrotreatment of West Texas VSR the viscosity of the resid at 60° C decreased from 324.8 to 1.07 poise; Conradson Carbon decreased by almost half and °API gravity almost doubled. The viscosities of the materials obtained from coprocessing have much lower viscosities than the original residuum. In the coprocessing reaction with a 10 to 1 solvent to coal ratio the viscosity was reduced to 0.363 poise and the Conradson Carbon was lowered to 13.49. The presence of the coal may be producing synergy in that the viscosity was reduced to less than that of West Texas VSR hydrotreated in the presence of NiMo/Al₂O₃ but in the absence of coal. Increased coal concentration resulted in an increase in the viscosity to 22.7 poise and an increase in Conradson Carbon to 17.78.

Effect of Hydrogen Donor Addition on Coprocessing

Recent studies have shown the importance of hydrogen donors and transfer agents in the dissolution of coal (8-11). The role and importance of hydrogen transfer in

coprocessing are investigated herein by studying the effect of the addition of hydrogen donor compounds such as tetralin, 1,2,3,4-tetrahydroquinoline (THQ) and 9,10-dihydrophenanthrene (DHP) to the petroleum solvent used in coprocessing. In these coprocessing reactions, the coprocessing solvent was Maya TLR and the coal was Illinois #6. Three levels of donable hydrogen have been studied, 0.15%, 0.55% and 1.5% in N₂ and H₂ atmospheres. The effect of these additions on oil production and coal conversion obtained from coprocessing reactions is presented in Table 3. In the coprocessing reactions in which tetralin was added, both coal conversion and oil production increased when comparing N₂ to H₂ atmospheres for equivalent donable hydrogen addition. However, at the 0.15% tetralin addition level in the H₂ atmosphere, the product slate was very similar to that obtained in H₂ using only Maya TLR. The effect of a H₂ atmosphere on coal conversion was dramatic, increasing coal conversion from 19.6% in N₂ to 58.9% in H₂ at the lowest donor hydrogen addition level. When 1.5% donable hydrogen was present in the tetralin Maya/TLR system, coal conversion in N₂ was 62.1% which was essentially equivalent to the coal conversion obtained with 0.15% donable hydrogen in a H₂ atmosphere. In these reactions, it appears that the form that the hydrogen is in, whether molecular hydrogen or donable hydrogen from hydroaromatic compounds, is not critical. The necessary criterion for coal conversion to be achieved is for the hydrogen to be present in a form which can be utilized by the coal. The use of a H₂ atmosphere to the tetralin/Maya TLR system with 1.5% donable hydrogen further aided in coal conversion, indicating that a hydrogen deficiency existed in the N₂ atmosphere even when a significant amount of tetralin was present.

As in the tetralin system, the effect of the H₂ compared to the N₂ atmosphere on the THQ/Maya TLR system was dramatic. At 0.15% donable hydrogen, coal conversion increased from 23.2% in N₂ to 58.0% in H₂. In contrast, coal conversion in the THQ/Maya TLR system at the highest donable hydrogen level was insensitive to atmosphere. In N₂, 89.0% coal conversion was observed while in H₂, 90.4%, was seen. The amount of pentane soluble materials produced was the same in N₂ regardless of the amount of donable hydrogen. In H₂, only a small increase in pentane solubles was observed by increasing the amount of donable hydrogen from 0.15% to 1.5%.

Oil production increased in the 1.5% donable hydrogen tetralin system compared to the 0.15% tetralin system. A possible reason for the increased oil production is the availability of more hydrogen to the dissolving coal matrix resulting in an increased amount of hydrogenation occurring and the production of hydrogenated products soluble in pentane. The change in solvent composition due to the presence of the hydroaromatic may also be partially responsible for the observed change in percent oil production. Further elucidation of the role of hydrogen donor compounds in coprocessing was sought by comparing the effect of DHP on the product slate to that of tetralin and THQ. The choice of DHP was based upon its comparable ability to convert coal as THQ (12) and upon the fact that it is a hydrocarbon without any of the detrimental characteristics generally associated with nitrogen containing hydroaromatics. When compared at a 0.55% donable hydrogen level, DHP converted more coal to soluble material than THQ and yielded a higher percent oil production than did tetralin.

Comparing the low levels of donable hydrogen using tetralin and THQ showed remarkably similar product distributions in both H₂ and N₂ atmospheres. A contrast is observed, however, when comparing these two at the highest donor level. In THQ, a markedly lower amount of pentane soluble material was produced than in tetralin. The percent oil production in the 1.5% donable hydrogen system in N₂ was -30.7% in THQ and 15.9% in tetralin; likewise, in H₂ the values were 4.0% in THQ and 25.0% in tetralin. The product slate obtained from THQ contained many more asphaltenes than that from tetralin.

These results are in agreement with those observed in coal liquefaction where hydroaromatics having a nitrogen functionality readily dissolve coal. The reasons for their effectiveness resulted from their ability to penetrate and swell coal and their ability to transfer hydrogen. These good features of the nitrogen containing compounds were, however, overridden by their propensity to form adducts with themselves and with coal-derived materials. This adduct formation has been extensively studied by Cronauer (13). The adduct formation is readily apparent in the increased levels of asphaltenes observed during the coprocessing reaction containing THQ.

Effect of Catalyst Type on Coprocessing

The effect of catalyst type on the coprocessing of heavy crudes and residua with coal has been investigated using a mineralogical pyrite and a small particle size NiMo on γ -Al₂O₃. Both of these catalysts were used to study their effect on upgrading residua and on the product slate from coprocessing. In the resid upgrading experiments, West Texas VSR was used; in the coprocessing reactions both West Texas VSR and Maya TLR were used. In Table 4, upgrading reactions of West Texas VSR are compared among the thermal reaction, the reaction containing pyrite and the reaction with small particle size NiMo/Al₂O₃ catalyst. The original solubility distribution obtained prior to reaction is given as a reference. Compared to the original West Texas VSR, the thermal reaction produced gases and IOM, lost oil, and increased slightly the amount of asphaltenes present. When pyrite was added as a catalyst, the asphaltenes were virtually eliminated from the residuum, producing primarily pentane soluble oil. Small amounts of gases, preasphaltenes and IOM were also produced. In contrast, the presence of a small particle size NiMo/Al₂O₃ catalyst did not change the oil fraction but did reduce the asphaltene fraction by ~80% producing gas, preasphaltenes and IOM in almost equal amounts.

The effect of pyrite and NiMo/Al₂O₃ addition on the products obtained from coprocessing are presented in Table 5. Four different reactions are compared with West Texas VSR: (1) thermal reaction (2) two reactions with pyrite and (3) reaction using small particle size NiMo/Al₂O₃. The conditions for all the reactions were the same; both pyrite and NiMo/Al₂O₃ were introduced at the same gram level. The pyrite reaction produced the most coal conversion, 87.6%, compared to 79.3% for the NiMo/Al₂O₃ and 55.0% for the thermal reaction. In terms of pentane soluble oils, the amount produced by the pyrite reaction fell between that obtained by the thermal reaction and by the commercial catalyst. Due to the effect observed on the residuum alone, pretreatment of the solvent with pyrite and hydrogen prior to using as a coprocessing solvent was thought to be possibly beneficial in improving the entire product slate. However, comparison of the product slate using the hydrotreated West Texas VSR to that obtained using the original showed little improvement that could be attributed to hydrotreatment. One possible explanation for this behavior is that the primary effect of the pyrite is in the upgrading of the residuum asphaltenes to pentane solubles and that the reaction producing pentane solubles from coal is not substantially affected by the presence of pyrite. Thus, the majority of the pentane solubles produced from the coprocessing reaction using the original West Texas VSR was produced most probably from the residuum and not from coal. In the hydrogen pretreatment case, most of the upgrading of the residuum had occurred prior to the coprocessing reaction leaving little material from the residuum for further upgrading. Consequently, little change in the product slate was observed between the original and hydrotreated material. When pyrite was used in coprocessing experiments using Maya TLR, similar results were obtained.

Single Stage and Two Stage Coprocessing Reactions

Two stage processing using sequential and possibly different catalysts in the first and second stages may produce a more favorable product slate from coprocessing as well as a more efficient use of hydrogen. Two sets of experiments were performed to investigate the effects of two stage processing and sequential catalytic treatment on coprocessing. One was a series of one hour reactions in which pyrite, NiMo/Al₂O₃ and H₂S were used individually as catalysts and in combination. These results are given in Table 6. In the second set two stage experiments were run for a total of one hour but after the first half hour the gases were vented, a new catalyst was added, and fresh hydrogen was charged. The catalyst charge at the end of both reactions was 2 grams.

The single stage one hour reactions showed similar results to that observed previously. The coprocessing reaction using pyrite catalyst again produced the highest coal conversion; however, the conversions observed from Shell 324 NiMo/Al₂O₃ were also both above 80%. The percent oil production observed is given below for the reactions containing the different catalyst

NiMo/Al₂O₃ > Pyrite + NiMo/Al₂O₃ > Pyrite > H₂S > Thermal 1)

The small particle size NiMo/Al₂O₃ is by far the most effective catalyst in producing pentane soluble oil.

To test the hypothesis that H₂S was the catalytic agent rather FeS₂ in the reactions using the pyrite catalyst, CS₂ which readily reacts with H₂ to form H₂S was added to the reaction. The amount of CS₂ added was equivalent to that needed to produce the same amount of H₂S as would be generated from FeS₂. Under these conditions, the product slate obtained did not vary significantly from the thermal reaction. This result suggests then that the important catalyst in the reactions using pyrite is the pyrite itself or its reduced form, not the evolved H₂S.

In two stage processing, four sets of experiments were performed: thermal for the first stage and thermal for the second stage; pyrite in both stages; then pyrite in the first stage with NiMo/Al₂O₃ in the second stage and NiMo/Al₂O₃ in both stages. The highest amount of coal conversion achieved, 92.2%, occurred in the experiments using pyrite in both stages. The pyrite/NiMo/Al₂O₃ and NiMo/Al₂O₃/NiMo/Al₂O₃ reactions also produced high coal conversions, 85.9% and 84.1%, respectively. The oil production from the two stage coprocessing showed the same order as did the single stage experiments. The reaction with NiMo/Al₂O₃ in both stages produced the most oil while the combination of pyrite/NiMo/Al₂O₃ was second.

Summary and Conclusions

In coprocessing, the solvent to coal ratio has a definite influence on the product distribution, oil production and coal conversion. The highest coal conversion occurred at a 50% coal concentration level and maximal oil production was achieved at 30 to 50% coal concentration. When reacted in a hydrogen atmosphere, the addition of hydrogen donor compounds to the coprocessing solvent definitely influenced the products from coprocessing. At equivalent donable hydrogen levels, DHP produced the highest coal conversion and oil production. At and above the 0.55% donable hydrogen level, THQ was very effective in converting coal but was detrimental to oil production. In general, the hydrogen donor compounds without heteroatoms appear to be more effective in producing oil than the nitrogen containing hydroaromatics.

The catalyst type is important in coprocessing since different catalysts influence different reactions in the two materials. Pyrite affected the upgrading of the residium by promoting the conversion of petroleum asphaltenes into oil. In coprocessing, the notable effect of pyrite was the reduction of the IOM levels and consequent increase in coal conversion. Compared to the thermal reaction, pyrite was effective in increasing the oil production in coprocessing. The small particle size NiMo/Al₂O₃ catalyst, however, was still more effective in hydrogenating the dissolving coal matrix and producing pentane soluble oil. In two stage processing, the combination of pyrite in the first stage and NiMo/Al₂O₃ in the second produced a much improved product slate compared to thermal processing. The highest oil production and coal conversion were, however, still achieved by using NiMo/Al₂O₃ in both stages.

References

1. Curtis, C. W., Pass, M. C. and Guin, J. A., submitted to I & EC Process Design and Development, 1984.
2. Yan, T. Y. and Espenschied, W. F., Fuel Processing Technology, 7, 121, 1983.
3. Shinn, J. H., Dahlberg, A. J., Kuehler, C. W., and Rosenthal, J. W., "The Chevron Co-Refining Process", presented at the EPRI Coal Liquefaction Contractor's Meeting, May 1984.
4. Moschopedis, S. E., Hawkins, R. W., Fryer, J. F. and Speight, J. G., Fuel, 59, 647, 1980.
5. Curtis, C. W., Tsai, K. J. and Guin, J. A., I & EC Process Design and Development, in press, 1985.
6. Miller, Ronald L., "Exploratory Studies in Co-Processing", EPRI Coal Liquefaction Contractor's Conference, May 1984.
7. Curtis, C. W., Guin, James A., Tarrer, Ray and Huang, Wan-Jiao, Fuel Process. Technology, 1983, 7, 277-291.
8. Neavel, R. C. Phil. Trans. R. Soc. Lond., 1981, A300, 141.
9. Brooks, D. G., Guin, J. A., Curtis, C. W. and Placek, T. D., Ind. Eng. Chem. Proc. Des. Dev. 1983, 22, 343.
10. Curran, G. P., Struck, R. T. and Gorin, E. Ind. Eng. Chem. Proc. Des. Dev., 1967, 6, 166.
11. Neavel, R. C., Fuel, 1976, 55, 234.
12. Curtis, C. W., Guin, J. A., Kwon, K. C., Fuel, 1984, 63, 1404.
13. Cronauer, D. D. Heterofunctionality Interaction with Donor Solvent Coal Liquefaction, " Fossil Energy Final Report for DOE|PC|50782-T1(DE840132-83).

Table 1
Analysis of Petroleum Solvents

Starting Materials	Oil	Asphaltenes	C	H	N	S	O by difference	Ash
Illinois #6 Coal			68.4	4.4	1.4	3.2	12.0	10.6
Maya TLR	79.5	20.5	85.3	10.8	0.51	4.19		0.082
West Texas VSR	86.2	13.8	86.1	10.4	0.44	3.33		0.012

Table 2
Physical Properties Comparison

Material Tested	Viscosity 60°C, poise	°API	Specific Gravity, 60°C	Conradson Carbon
West Texas VSR	324.8	7.9	1.015	16.4
Product from 10:1 West Texas VSR to Coal Coproprocessing Reaction	0.363	13.39	0.9766	13.49
Product from 2:1 West Texas VSR to Coal Coproprocessing Reaction	22.7	7.1	1.021	17.78
Hydrotreated West Texas VSR	1.07	15.9	0.96	9.34

Table 3
Effect of Hydrogen Donor Addition on Coprocessing

	Oil Production, %		Coal Conversion, %	
	H ₂	N ₂	H ₂	N ₂
Maya TLR	11.8	-11.6	60.0	24.1
0.15% Donable Hydrogen Added				
Tetralin	11.2	- 9.2	58.9	19.6
THQ	6.7	-12.3	58.0	23.2
0.55% Donable Hydrogen Added				
Tetralin	10.5	0.7	58.8	39.3
THQ	2.5	-11.4	75.4	52.7
9,10-DHP	17.5	4.6	81.0	58.8
1.5% Donable Hydrogen Added				
Tetralin	25.0	15.9	81.0	62.1
THQ	4.0	-30.7	90.4	89.0

Table 4
Effect of Catalyst on Upgrading of West Texas VSR

	West Texas VSR Original	West Texas VSR	West Texas VSR	West Texas VSR
Catalyst	NA	None	Pyrite	NiMo/Al ₂ O ₃
Coal	NA	None	None	None
Gas	0.0	3.5	1.9	3.9
Oil	86.2	79.1	95.3	86.6
Asphaltenes	13.8	15.0	0.6	3.1
Preasphaltenes	0.0	0.1	1.2	2.8
IOM	0.0	2.3	1.0	3.6
H ₂ Consumption, %	NA*	4.9	15.4	31.9

*NA: not applicable

Reaction Time: 30 minutes

Table 5
Effect of Catalyst on the Coprocessing Reactions

Catalyst	West Texas	West Texas	Hydrotreated*	West Texas
	VSR Original	VSR	West Texas	VSR
	None	Pyrite	Pyrite	NiMo/Al ₂ O ₃
Gas	4.2	3.3	3.0	4.3
Oil	58.6	67.1	68.3	72.9
Asphaltenes	15.2	19.6	16.6	13.4
Preasphaltenes	8.2	6.2	6.6	3.0
IOM	13.8	3.8	5.5	6.4
Coal Conversion, %	55.5	87.6	82.3	79.3
H ₂ Consumption, %	24.2	37.9	30.0	52.9
Oil Production, %	-2.1	18.8	2.25	33.1

*The solvent was hydrotreated in the presence of pyrite.

Catalyst	Maya TLR	Maya TLR	Maya TLR
	None	Pyrite	NiMo/Al ₂ O ₃
Gas	4.3	3.3	4.7
Oil	60.1	64.6	69.7
Asphaltenes	14.7	19.1	16.4
Preasphaltenes	8.5	7.1	2.2
IOM	12.4	5.9	7.1
Coal Conversion, %	60.0	81.0	77.0
H ₂ Consumption, %	18.9	40.1	55.6
Oil Production, %	11.7	21.5	32.9

Table 6
Single Stage Coprocessing Using West Texas VSR

Catalyst	Thermal	~0.32g CS ₂	Pyrite	NiMo/Al ₂ O ₃	Pyrite & NiMo/Al ₂ O ₃
Coal Conversion, %	58.2	57.4	89.2	85.0	83.7
Hydrogen Consumption, %	30.4	33.3	57.1	72.5	66.5
Oil Production, %	-8.3	-6.9	23.9	54.3	39.3

Two Stage Coprocessing Using West Texas VSR

First Stage Catalyst	None	Pyrite	Pyrite	NiMo/Al ₂ O ₃
Second Stage	None	Pyrite	NiMo/Al ₂ O ₃	NiMo/Al ₂ O ₃
Coal Conversion, %	64.3	92.2	85.9	84.1
Hydrogen Consumption, %	14.5	27.5	35.6	41.1
Oil Production, %	-0.4	26.8	43.0	58.5

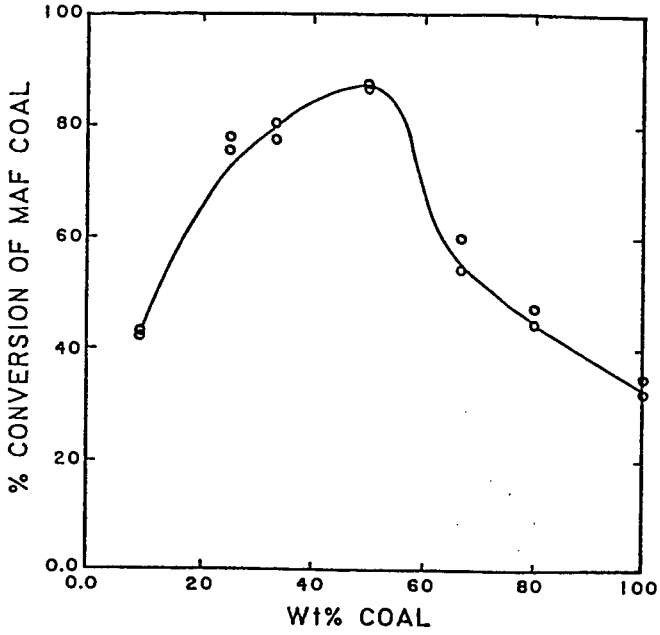


Figure 1. Coal Conversion as a Function of Coal Concentration

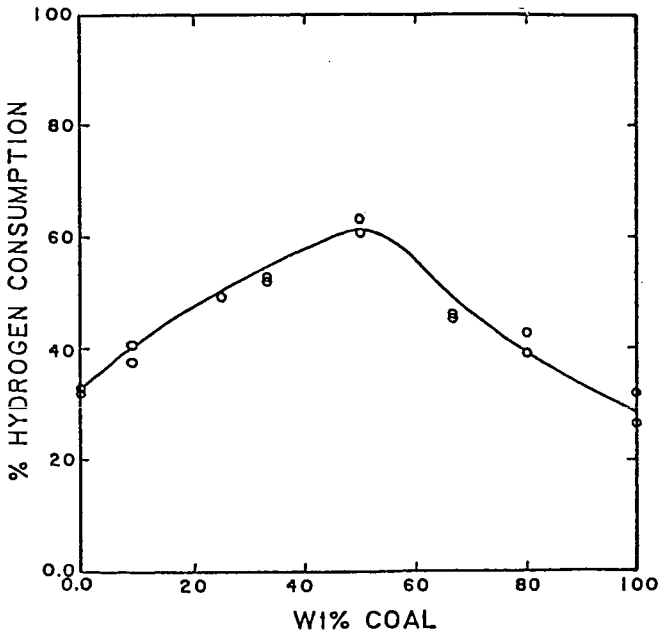


Figure 2. Hydrogen Consumption as a Function of Coal Concentration

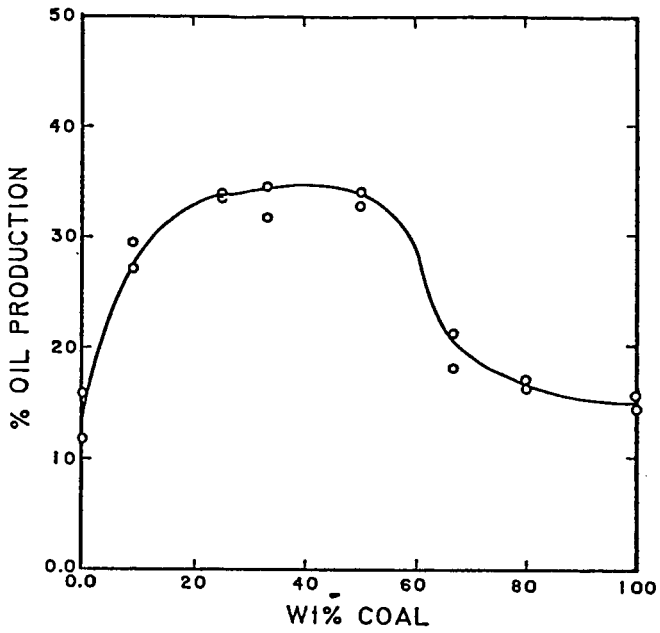


Figure 3. Oil Production as a Function of Coal Concentration

HIGH-PRESSURE CATALYTIC HYDROPROCESSING
OF A
SIMULATED COAL LIQUID

By

M. J. Girgis, B. C. Gates
Center for Catalytic Science and Technology, Department of Chemical Engineering
University of Delaware, Newark, Delaware 19716

and
L. Petrakis
Gulf Research and Development Company, Pittsburgh, Pennsylvania 15320

INTRODUCTION

The catalytic hydroprocessing of coal-derived liquids is poorly understood because of the complexity of the liquids and the large number of competing reactions. The goal of this research was to characterize quantitatively the hydroprocessing of a liquid mixture modelling a coal liquid derived from Powhatan No. 5 coal in the SRC-II process. A specific goal was to determine relative reactivities of representative reactants and determine the competitive inhibition effects of the various reactants. The experiments were carried out with a mixture of at most nine compounds representing the major functional groups in the coal liquid. The reactants included polynuclear aromatic hydrocarbons, sulfur- and oxygen-containing heterocyclics, 1-naphthol, and basic as well as nonbasic organonitrogen compounds.

There is no one typical coal liquid because the compounds and their relative amounts vary with the source of the coal and with the type and operating severity of the coal liquefaction process. In this study, the choice of model compounds and their relative amounts were based on a detailed analysis of the SRC-II heavy distillate (1,2). The concentrations of compounds containing heteroatoms were chosen to give the same concentrations of functional groups present in the SRC II heavy distillate; the concentrations of aromatic hydrocarbons were chosen to give a molar ratio of 3:2:1 of fused 2-ring, 3-ring, and 4-ring aromatic compounds.

EXPERIMENTAL

Apparatus and Procedure

The experiments were carried out with a fixed-bed flow microreactor (3). The feed was prepared by dissolving the reactant compounds in cyclohexane to give a solution with a total solute mass fraction of 0.0025. Approximately 800 ml of solution was added to either of two 1000-ml high-pressure autoclaves equipped with stirrers. The feed and the vapor space above it were purged with hydrogen for two hours at room temperature with a hydrogen flow rate of 50 ml/min. Carbon disulfide dissolved in another 10 ml of feed was then quickly added to give 0.001 mass fraction of carbon disulfide in the feed. [The carbon disulfide served as a source of hydrogen sulfide via the reaction $CS_2 + 4H_2 \longrightarrow 2H_2S + CH_4$, which occurs rapidly under the reaction conditions (4); the CS_2 maintained the catalyst in the sulfided state.] The autoclave was pressured up to 137.1 atm with hydrogen at room temperature, and the feed was saturated with hydrogen. This resulted in a hydrogen mole fraction of approximately 0.05 in the feed (5) or a 50:1 hydrogen to reactant mole ratio, which prevented the hydrogen mole fraction from varying significantly over the length of the reactor.

The saturation of the feed with hydrogen prior to its introduction into the reactor ensured that only two phases were present in the reactor, which allowed

determination of reaction kinetics in the absence of mixing effects or significant radial gradients in concentration or temperature. Because the reactor was held at a higher temperature and pressure than the autoclave, no degassing of the feed occurred, as confirmed by thermodynamic calculations.

The reactor consisted of a vertical 316 stainless steel tube 25.4 cm long with an internal diameter of 0.95 cm. The bottom 11 cm of the reactor were packed with 90-mesh alundum, the next 3 cm were packed with 0.050 g of catalyst mixed with alundum, and the remainder of the tube was packed with alundum. A detailed description of the reactor is given elsewhere (3).

The catalyst was sulfided by passing a mixture of 10% H₂S in H₂ through the catalyst bed at 30 cm³/min for two hours at 400°C. The reactor was then cooled to the reaction temperature (usually 350°C) under H₂S/H₂ and then brought to the reaction pressure of 171 atm. The feed was pumped through the reactor by a Waters M-6000A liquid chromatography pump. Liquid samples could be taken from either a sampling valve or a dead volume cylinder, both of which were located downstream of the reactor. For each run, the reactor was operated until steady-state was reached (usually 24-30 h); only data from steady-state samples are reported.

The analyses of the liquid samples were performed with a Tracor 560 gas chromatograph (GC) equipped with a 30-m DB-5 bonded phase capillary column. The GC contained an outlet splitter which permitted the column effluent to be divided into two streams, one going to a flame ionization detector (FID) and the other to a Hall electrolytic conductivity detector. The latter was used to identify nitrogen-containing compounds and the former was used for quantitative product analysis using *n*-decane as an internal standard. FID response factors relative to *n*-decane were determined for all the reactants. Some of the samples were also analyzed by gas chromatography-mass spectrometry.

Materials

The catalyst used in this work was American Cyanamid HDS-9A, a NiO-MoO₃/γ-Al₂O₃ catalyst, the properties of which are listed in Table II. Prior to use, the catalyst was ground from 1/16" extrudates to 80-100 mesh particles. The alundum used to pack the reactor was Alundum RR (Fisher Scientific, Blue Label). All chemicals listed in Table I as well as the cyclohexane solvent were obtained from Aldrich Chemical Company and used as received. *n*-Decane was obtained from Eastman Chemical Co. High-pressure hydrogen (3500 psig) and the 10% H₂S in H₂ were obtained from Linde and Matheson, respectively.

RESULTS AND DISCUSSION

The first series of experiments was conducted with the simulated coal liquid designated in Table I. These experiments had the following objectives:

- a) To determine the reactivities of the various reactants in a mixture at different temperatures and weight hourly space velocities (WHSV).
- b) To identify as many reaction products as possible.
- c) To establish the limitations of the chromatographic analyses of the products (e.g., determine which peaks could not be resolved). Product chromatograms were expected to be complex, with overlapping peaks.

Experiments were carried out at each of the conditions shown in Table III. In Table IV, the reaction products identified are listed with the methods used to identify them (mass spectrometry and co-injection with a pure compound into the chromatograph). Some problems were encountered in resolving important peaks in the product chromatograms. The major resolution difficulty occurred with dibenzothiophene; a peak of comparable size was merged with it on its down slope, and a small peak from a nitrogen-containing compound appeared on its up slope. The small peak on the up slope was not resolvable from the dibenzothiophene peak on the FID trace (we detected it with the Hall detector); as a result, the calculated dibenzothiophene mass fraction was greater in product samples than in

the feed. Therefore, the only way to determine dibenzothiophene hydrodesulfurization (HDS) was to sum the mass fractions of biphenyl and cyclohexylbenzene in the product and divide by the feed dibenzothiophene mass fraction. A similar difficulty occurred with phenanthrene, as the Hall detector indicated a nitrogen-containing peak at approximately the retention time of phenanthrene, whereas the FID trace showed only one large peak. Since the Hall detector was used only for qualitative analysis, it was not possible to subtract the contributions of the nitrogen-containing compounds. Hence, we expect that the actual phenanthrene conversion was somewhat higher than the calculated results. The additional analytical problem occurred with acridine. Of the approximately six organonitrogen compound peaks expected as acridine products, only one, that for 1,2,3,4,5,6,7,8-octahydroacridine, was identified; no hydrocarbon hydrodenitrogenation (HDN) products were identified.

Table V is a summary of the results for runs at constant temperature (350°C) and varying WHSV with the simulated coal liquid designated in Table I. The conversions of the basic nitrogen compounds, quinoline and acridine, were higher than that of indole, the non-basic nitrogen compound. However, the fraction HDN of quinoline (defined as the moles of the quinoline and nitrogen-containing quinoline derivatives in the product divided by the moles of quinoline in the feed) was considerably less than the quinoline conversion. It was not possible to obtain a reliable value for acridine HDN.

Figure 1 is a pseudo first order kinetics plot for quinoline and indole HDN (i.e., a plot of the fraction of non-dehydrodenitrogenated compounds vs. inverse space velocity). Quinoline HDN followed pseudo first order kinetics, whereas indole HDN did not.

The conversion of dibenzofuran was too low to be measured reliably; this was the least reactive of the reactants. In contrast, the conversion of 5,6,7,8-tetrahydro-1-naphthol was always greater than 80%. No oxygen-containing products of 5,6,7,8-tetrahydro-1-naphthol were found; it is inferred that the 5,6,7,8-tetrahydro-1-naphthol conversion is identical to its hydrodeoxygenation (HDO).

Dibenzothiophene was converted appreciably only at the lowest space velocity; biphenyl and cyclohexylbenzene were detected as HDS products.

The conversions of phenanthrene, fluoranthene, and pyrene were, in order of decreasing reactivity: fluoranthene > pyrene > phenanthrene. As a consequence of the nitrogen compound peak that was merged with that of phenanthrene, the actual phenanthrene conversion is inferred to have been higher than that shown in Table V. The pseudo first order kinetics plots for these three hydrocarbons suggest that the hydrogenation reactions were reversible, as expected.

Table VI is a summary of runs made at constant space velocity but with the temperature varied from 300 to 400°C with the simulated coal liquid designated in Table I. A sharp increase in quinoline HDN was observed from 300 to 350°C. However, the quinoline HDN hardly changed from 350 to 400°C; the product quinoline mass fraction observed in the run at 400°C was approximately five times that observed at 350°C, which is consistent with earlier observations that quinoline hydrogenations are reversible (6).

The HDN trend with indole was rather different: the large change in HDN occurred from 350 to 400°C, whereas the HDN was practically unchanged from 300 to 350°C; inspection of the indole mass fraction in these runs (Table VI) reveals that the indole conversion paralleled that of the HDN, suggesting that nitrogen-containing intermediates of indole were more reactive than indole itself.

The reactivities of the two oxygen compounds were at extremes: dibenzofuran conversion was low, even at the highest temperature, while the HDO of 5,6,7,8-tetrahydro-naphthol was complete at 350°C. As for dibenzothiophene, the HDS increased with temperature, with the largest change occurring from 350 to 400°C.

Phenanthrene conversion also increased with temperature. However, fluoranthene and pyrene gave a different result: in each case conversion

increased from 300 to 350°C but decreased significantly from 350 to 400°C. The decrease in conversion suggests that pyrene and fluoranthene hydrogenations are rapid but limited strongly by equilibrium at the highest temperature.

From the data presented in Tables V and VI it is evident that the conversions of dibenzothiophene, dibenzofuran, and the aromatic hydrocarbons were all low compared with those of the other compounds. In addition, organonitrogen compounds and water (one of the products of 5,6,7,8-tetrahydro-1-naphthol HDO) are known inhibitors (7, 8). These findings motivated the next set of experiments using another simulated coal liquid, Table VII. This simulated coal liquid contains the same mass fractions of dibenzofuran, dibenzothiophene, and the three aromatics as the one designated in Table I, with the nitrogen compounds and 5,6,7,8-tetrahydro-1-naphthol removed.

Experiments were carried out at 350°C and at WHSV with the simulated coal liquid designated in Table VII, and the results are summarized in Table VIII. The results of Figure 2 suggest that the hydrogenations of fluoranthene and pyrene were reversible; phenanthrene appeared to follow pseudo first order kinetics. Dibenzofuran conversion was again very low, suggesting that its low reactivity

— referred to above—was not the result of inhibition by organonitrogen compounds and/or water. On the other hand, dibenzothiophene HDS was markedly greater in this coal liquid compared with the one designated in Table I. It is especially instructive to compare the results from Run 6 (Table VIII) with those from Run 1 (Table VI) as both runs were made with the same catalyst loading, feed flow rate, and the same mass fractions of dibenzofuran, dibenzothiophene, phenanthrene, fluoranthene, and pyrene. The inhibition effect of the organonitrogen inhibitors and/or the 5,6,7,8-tetrahydro-1-naphthol was strong for all the reactants except dibenzofuran.

Additional experiments are planned where 5,6,7,8-tetrahydro-1-naphthol, indole, and quinoline will be subsequently added to the simulated coal liquid specified in Table VII; these should give additional information concerning the cause of the inhibition in the runs with the simulated coal liquid given in Table I.

ACKNOWLEDGMENTS

The experimental assistance of S. K. Starry and S. A. Wikoff is gratefully acknowledged. This work was supported by DOE.

REFERENCES

1. Petrakis, L., D. C. Young, R. G. Ruberto, and B. C. Gates, *Ind. Eng. Chem. Process Des. Dev.* 1983, 22, 298.
2. Gates, B. C., J. H. Olson, G. C. A. Schuit, A. B. Stiles, and L. Petrakis, "Kinetics and Mechanism of Catalytic Hydroprocessing of Components of Coal-derived Liquids," United States Department of Energy Report No. DE-AC22-79ET14880-17, January 17, 1984.
3. Eliezer, K. F. *et al.*, *Ind. Eng. Chem. Fundam.*, 1977, 16, 380.
4. Sapre, A. V., Ph.D. dissertation, University of Delaware, Newark, Delaware, 1981.
5. Berty, T. E., H. H. Reamer, and B. H. Sage, *J. Chem. Eng. Data*, 1966, 11 (1), 25.
6. Satterfield, C. N. and S. H. Yang, *Ind. Eng. Chem. Process Des. Dev.*, 1984, 23, 11.
7. Bhide, M. V., Ph.D. dissertation, University of Delaware, Newark, Delaware, 1979.
8. Lipsch, J. M. J. G. and Schuit, G. C. A., *J. Catal.*, 1969, 15, 174.

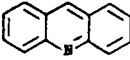
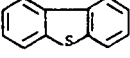
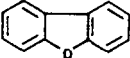
TABLE I			
	SIMULATED	COAL	LIQUID
COMPOUND	STRUCTURE	COMPOUND CLASS	RELATIVE MOLE FRACTION
Quinoline			Basic Nitrogen 0.0265
Acridine			Basic Nitrogen 0.0261
Indole			Nonbasic Nitrogen 0.0384
Dibenzothiophene			Sulfur Heterocyclic 0.0347
Dibenzofuran			Oxygen Heterocyclic 0.0639
5,6,7,8-tetrahydro-1-naphthol			Naphthol 0.1133
Fluorene			Fused two-ring Aromatic 0.3489
Phenanthrene			Fused three-ring Aromatic 0.2320
Pyrene			Fused four-ring Aromatic 0.1163

TABLE II
PROPERTIES OF AMERICAN CYANAMID¹ HDS-9A CATALYST

Composition, wt. %	
SiO ₂	3.1
SnO ₃	18.3
WO ₃	0.04
Na ₂ O	0.05
Surface Area, m ² /g	149
Pore Volume, cm ³ /g	0.51

1. The reported values were determined by the catalyst manufacturer.

TABLE III
CONDITIONS OF FIRST SET OF EXPERIMENTS

PRESSURE = 171 ATMOSPHERES

RUN #	TEMPERATURE, °C	WHSV, (g of reactants)/(g of catalyst h)
1	350	0.99
2	350	2.17
3	350	4.14
4	400	1.03
5	300	1.10

TABLE IV PRODUCT IDENTIFICATIONS

REACTANT	PRODUCTS	METHODS OF IDENTIFICATION	
		Co-injection in GC	Mass Spectrometry
Quinoline	1,2,3,4-tetrahydroquinoline	x	
	5,6,7,8-tetrahydroquinoline	x	
	Decahydroquinoline	x	
	2-propylaniline	x	
	Propylbenzene	x	
	Propylcyclohexane	x	
Indole	Indoline	x	
	2-ethyl aniline	x	
	Ethylbenzene	x	
	Ethylcyclohexane	x	
5,6,7,8-Tetrahydro-1-naphthol	Tetralin	x	x
	cis-Decalin	x	*
	trans-Decalin	x	x
	Naphthalene	x	x

*Identified as octahydromethylindan by mass spectrometry.

Dibenzotbiophene	Biphenyl	x	x
	Cyclohexylbenzene	x	x
Phenanthrene	Dihydrophenanthrene		x
	Octahydrophenanthrene		x
Acridine	1,2,3,4,5,6,7,8-Octahydroacridine	x	
Fluoranthene	1,2,3,10a-Tetrahydrofluoranthene		x
Pyrene	Dihydropyrene (isomer unidentified)		x
	Hexahydropyrene (isomer unidentified)		x

TABLE V
SUMMARY OF RESULTS OBTAINED AT T=350C AND VARIABLE WHSV

FEED: SIMULATED COAL LIQUID DESIGNATED IN TABLE I

RUN #	1	2	3
WHSV, (g of reactants)/(g of cat h)	0.99	2.17	4.14
PERCENTAGE CONVERSION			
QUINOLINE	97.9	90.7	88.2
INDOLE	46.4	29.9	22.9
5,6,7,8-TETRAHYDRO-1-NAPHTHOL	100	82.4	82.5
DIBENZOFURAN	4.1	7.5	0.0
DIBENZOTHIOPHENE	15.4	0.0	0.0
PHENANTHRENE	9.9	9.3	7.3
ACRIDINE	72.3	91.9	92.2
FLUORANTHRENE	41.7	24.9	23.1
PYRENE	20.3	16.6	18.8
QUINOLINE PERCENTAGE HDN	59.6	33.0	15.7
INDOLE PERCENTAGE HDN	27.8	19.7	13.5

TABLE VI
SUMMARY OF RESULTS OBTAINED AT WHSV=1 AND VARIOUS TEMPERATURES

FEED: SIMULATED COAL LIQUID DESIGNATED IN TABLE I

RUN #	5	1	4
TEMPERATURE, C	300	350	400
WHSV, (g of reactants)/(g of cat h)	1.1	0.99	1.03
PERCENTAGE CONVERSION			
QUINOLINE	98.8	97.9	88.4
INDOLE	43.0	46.4	70.5
5,6,7,8-TETRAHYDRO-1-NAPHTHOL	59.8	100	99.9
DIBENZOFURAN	0.9	4.1	5.1
DIBENZOTHIOPHENE	0.0	15.4	75.9
PHENANTHRENE	3.9	9.9	13.8
ACRIDINE	87.7	72.3	75.9
FLUORANTHRENE	30.4	41.7	16.2
PYRENE	12.8	20.3	13.6
QUINOLINE PERCENTAGE HDN	4.2	59.6	54.3
INDOLE PERCENTAGE HDN	27.5	27.8	55.0

TABLE VII

COMPOSITION OF SECOND SIMULATED COAL LIQUID

COMPOUND	RELATIVE MOLE FRACTION
Dibenzofuran	0.0807
Dibenzothiophene	0.0437
Fluoranthene	0.4396
Phenanthrene	0.2921
Pyrene	0.1454

TABLE VIII
SUMMARY OF RESULTS OBTAINED WITH THE
SIMULATED COAL LIQUID DESIGNATED IN TABLE VII

RUN #	6	7
TEMPERATURE, C	350	350
PRESSURE, ATM	172	173
WHSV, (g of reactants)/(g of cat h)	0.84	1.73

PERCENTAGE CONVERSION		
DIBENZOFURAN	2.8	2.7
DIBENZOTHIOPHENE	30.7	10.3
PERANTHRENE	33.1	18.0
FLUORANTHRENE	65.6	48.6
PYRENE	37.7	27.6

FIGURE 1
QUINDLINE AND INDOLE PERCENT HON

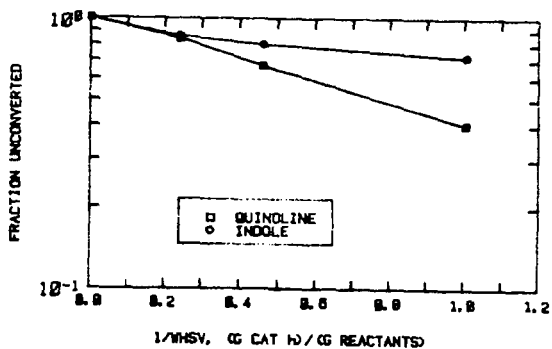
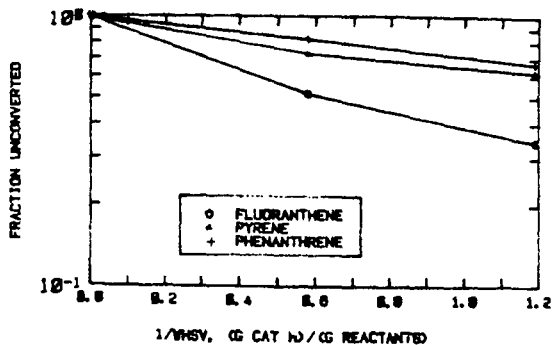


FIGURE 2
REACTIVITIES OF AROMATICS



A LABORATORY STUDY OF
AGGLOMERATION IN COAL GASIFICATION

C. R. Hsieh and P. T. Roberts

Chevron Research Company, Richmond, California 94802-0627

INTRODUCTION

The agglomerating tendencies of coal during gasification, especially during various stages of reaction, is a complex reaction.

Several investigators have studied the behavior of carbon-free ash. Stallmann and Neavel (1) found that the agglomerates of fused ash appear to form at temperatures below the initial deformation temperature, as defined by the ASTM fusibility test (2). Huffman, et al. (3) observed that significant particle melting of the ashes occurred at temperatures as much as 200-400°C below the ASTM initial deformation temperature. They also noted that melting was greatly accelerated under reducing conditions. Rehmat and Saxena (4) argued that it is not necessary for every reacting particle to attain the ash fusion temperature in order for agglomeration to occur. Only a few particles are required to reach the ash melting temperature. These particles form the nuclei for the formation of the ash agglomerates, and this process will indeed consume the ash produced from other particles.

In a fluidized bed, Langston and Stephens (5) recognized that the defluidizing tendency or the stickiness of the particles is directly proportional to the area of contact, the adhesive property of the particles, and inversely proportional to their momentum. Mason and Patel (6) felt that agglomeration depends on fluidized bed temperature, bed ash concentration, average particle size, superficial velocity, and bed height. Goldberger (7) and Siegell (8) both found that the ash softening temperature had no effect on the defluidization characterization for ash samples in their experiments. Basu (9) concluded that defluidization of a fluid bed is governed by the sintering characteristics of the bed material.

In some gasification processes, however, the carbon is only partially gasified in a reducing atmosphere and the remaining carbon is oxidized in a separate combustion zone (10). In addition, an inert solid is present which serves as a heat carrier and a diluent for the coal. The agglomerating tendencies of coal in such a process are different from the behavior of carbon-free ash.

In this paper, we have evaluated the agglomeration of coal, char, and ash during various stages of reaction. This included a range of temperatures, under reducing and oxidizing conditions, and in a mixture with an inert solid.

EXPERIMENTAL

Sample Preparation - Table I shows the proximate and the ultimate analyses of the three subject coals. Table II summarizes the mineral analyses of the ashes which were generated by heating the

coals in air to 538-649°C and screening all samples to pass between 100-mesh and 200-mesh U.S. standard screen. When sand was used, it was 16-30 mesh.

TABLE I
COAL ANALYSIS

	North Dakota <u>Lignite</u>	Western <u>Subbituminous</u>	
		<u>No. 1</u>	<u>No. 2</u>
Proximate Analysis, %			
Moisture	12.3	11.3	8.0
Volatile	34.5	31.3	13.0
Fixed Carbon	44.2	40.2	60.0
Ash	9.1	17.2	19.0
Ultimate Analysis, %			
H ₂ O	12.3	11.3	8.0
C	60.2	54.8	64.9
H	4.2	4.1	2.0
N	0.9	1.1	0.9
S	1.0	0.8	2.6
O	12.3	10.8	2.5
Ash	9.1	17.2	19.0

TABLE II
MINERAL ANALYSIS OF ASH

<u>% of Ash</u>	North Dakota <u>Lignite</u>	Western <u>Subbituminous</u>	
		<u>No. 1</u>	<u>No. 2</u>
SiO ₂	39.8	59.3	23.8
Al ₂ O ₃	16.4	25.7	9.2
TiO ₂	0.8	0.9	0.5
Fe ₂ O ₃	8.1	5.2	14.3
CaO	13.0	2.7	14.2
MgO	3.9	1.0	4.5
K ₂ O	0.2	0.8	0.5
Na ₂ O	0.8	1.9	5.9
SO ₃	15.9	2.2	26.6
P ₂ O ₅	0.5	0.2	0.2
SrO	0.4	0.0	0.1
BaO	0.1	0.1	0.3
Mn ₃ O ₄	0.2	0.0	0.1

Equipment and Procedures - Figure 1 shows the experimental setup employed. In a typical experiment, the furnace was purged with nitrogen and preheated to 538°C before a 0.5-g sample of material was placed in a ceramic boat and positioned in the center of the furnace. The sample was heated to the desired temperature in nitrogen before either a reducing or an oxidizing gas was passed over the sample for a predetermined time. The gas flow velocity was approximately 0.8 cm/sec. After each experiment, the sample was allowed to cool outside the furnace and sieved to determine the extent of agglomeration. The extent of agglomeration is defined as the weight percent retained on a mechanically vibrated 100-mesh screen.

The oxidizing gas was air. The reducing gas consisted of 51.8 vol % H₂, 25.8 vol % CO, 18.8 vol % H₂O, 1.7 vol % H₂S, 1.1 vol % CO₂, and 0.8 vol % NH₃. In some experiments, water was not used.

The average mass balance varied from a low of 96.9% for the North Dakota Lignite ash to a high of 100.8% for the Western Subbituminous No. 1, assuming complete decomposition of the sulfate and phosphate from the ash under experimental conditions.

In either a reducing or an oxidizing atmosphere at a given temperature, run lengths between 10 min. and 30 min. caused no significant difference in agglomeration, indicating that the agglomeration is complete by 10 min. Varying the sample size from 0.5-1.5 g showed no significant difference in the results, indicating that there is no particle mass transfer limitation in our tests.

RESULTS

Ash Agglomeration - Figure 2 shows the results with carbon-free ashes in the reducing gas. At 927°C, there is no significant agglomeration of any of the samples. The Western Subbituminous No. 1 sample developed substantial agglomeration at 982-1038°C, the No. 2 sample at 1038-1093°C, and the North Dakota Lignite ash at 1093-1149°C. All three samples were completely agglomerated at 1149°C. Figure 3 shows that in a reducing environment, the agglomerates transformed from a loosely packed ash at low temperature to a glassy melt at high temperature.

Figure 4 shows the effects of both reducing and oxidizing environments at 1149°C. Both conditions produce agglomeration, but at this temperature the reducing gas leads to more pronounced agglomeration. There was no agglomeration in a nitrogen environment. Thus, agglomeration is related to reactions between components in the ash and in the surrounding gas environment.

Effect of Carbon Conversion - Western Subbituminous Coal No. 1 was used to prepare samples of varying carbon content. The samples were tested in a variety of environments. Figure 5 shows that the agglomeration tendency correlates well with carbon content. No agglomeration occurs until more than 80% of the carbon is removed. Thus, modest amounts of carbon will retard ash agglomeration, even at quite severe conditions. Figure 6 shows that at 64%

carbon conversion, the sample looks much like the starting coal. At 99% conversion, the sample has agglomerated some, but still not to the extent as a carbon-free ash.

Effect of Inert Solids - Since carbon-free ash samples agglomerated the most, we mixed them with silica sand at a 1/10 ratio. Table III shows that agglomeration decreased in both reducing and oxidizing environments. Figure 7 shows that this decrease in agglomeration is quite dramatic in the reducing atmosphere. The ash samples agglomerated and shrunk; on the other hand, the particles in the ash/sand mixtures are well separated and bulky.

TABLE III
AGGLOMERATION OF
WESTERN SUBBITUMINOUS NO. 1

	% Agglomeration		
	1038°C	1093°C	1149°C
Ash Only			
N ₂	0	0	0
Reducing, 10 Min.	74	97	100
Oxidizing, 10 Min.	78	98	100
Oxidizing, 30 Min.	74	99	100
Ash + Sand			
N ₂	1	1	2
Reducing, 10 Min.	64	94	91
Reducing, 30 Min.	65	86	91
Oxidizing, 30 Min.	13	60	87

DISCUSSION

Agglomeration Temperature - Stallmann and Neavel (2) defined the agglomeration temperature as the 50% point on a curve like those in Figure 2, which corresponds to the steep part of these curves. Figure 8 compares the agglomeration temperature from both our experiments and those of Stallmann and Neavel (2) with the ASTM initial deformation temperature. This figure confirms the observations made by Stallmann and Neavel that the agglomeration temperature is a few hundred degrees lower than the ASTM temperature and that the ASTM initial deformation temperature cannot be correlated to the agglomeration temperature.

Figure 9 indicates that the agglomeration temperature for these three coal ashes decreases linearly with increasing sodium content of the ash. No other ash component showed a consistent relationship to agglomeration.

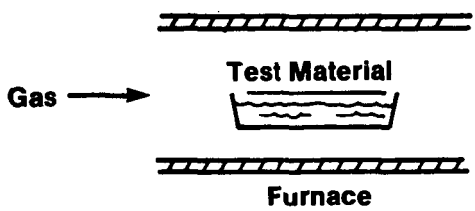
Process Implications - The control of agglomeration is important in the design and operation of a coal gasification or combustion process. We found that agglomeration depends on both coal

properties and on process conditions. In particular, the agglomeration of partially converted coal is negligible up to 80 wt % conversion. At higher conversions, agglomeration could be controlled by diluting the reacting material with inert materials such as sand. This study also indicated that agglomeration occurs on a shorter time scale than the nominal residence time in all but the most kinetically rapid gasification systems. These observations suggest that a gasification process which requires only partial gasification in a reducing atmosphere and which employs a diluent inert, such as the one disclosed by Mitchell, et al. (10), can greatly reduce the agglomeration problem which may occur in processing coal.

LITERATURE CITED

- (1) Stallmann, J. J. and Neavel, R. C., "Techniques to Measure the Temperature of Agglomeration of Coal Ash," *Fuel*, Vol. 59, 584 (1980).
- (2) Am. Soc. Test Mat., "Fusibility of Coal and Coke Ash," ASTM D 1857-68 (Reapproved 1980).
- (3) Huffman, G. P., Huggins, F. E., and Dunmyre, G. R., "Investigation of the High Temperature Behavior of Coal Ash in Reducing and Oxidizing Atmospheres," *Fuel*, Vol. 60, 585 (1981).
- (4) Rehmet, A. and Saxena, S. C., "Agglomeration of Ash in Fluidized Bed Gasification of Coal by Steam-Oxygen (or Air) Mixture," *Ind. Eng. Chem., Process Design Develop.*, 19, 223 (1980).
- (5) Langston, B. G. and Stephens, F. M., "Self-Agglomerating Fluidized Bed Reduction," *J. Metals*, April, 312 (1960).
- (6) Mason, D. M. and Patel, J. G., "Chemistry of Ash Agglomeration in the U-Gas Process," *Fuel Proc. Tech.*, 3, 181 (1980).
- (7) Goldberger, W. M., "Collection of Fly Ash in a Self-Agglomerating Fluidized Bed Coal Burner," ASME paper, 67 WA/FU-3, November 1967.
- (8) Siegell, J. H., "Defluidization Phenomena in Fluidized Beds of Sticky Particles at High Temperature," Ph.D. Dissertation, The City University of New York, 1976.
- (9) Basu, P., "A Study of Agglomeration of Coal Ash in Fluidized Beds," *Can. J. Ch.E.*, 60, 791 (1982).
- (10) Mitchell, D. S. and Sageman, D. S., "Countercurrent Plug-like Flow of Two Solids," U.S. Patent 4,157,245, June 5, 1979.

FIGURE 1
ASH AGGLOMERATION TEST



Initial Material
100-200 Mesh

Agglomeration
Material Retained on a 100 Mesh Screen
After Test Expressed as Wt % Ash

FIGURE 2
ASH AGGLOMERATION IN REDUCING GAS

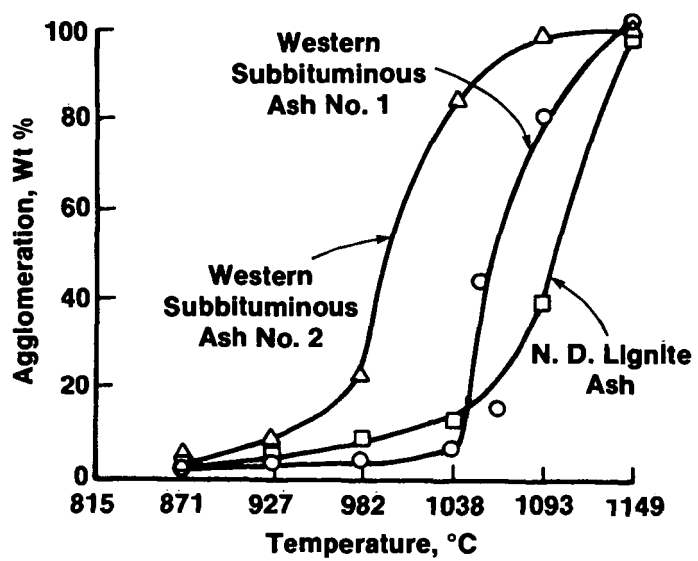


FIGURE 3
EFFECT OF TEMPERATURE ON
AGGLOMERATION



1038°C, Reducing Gas

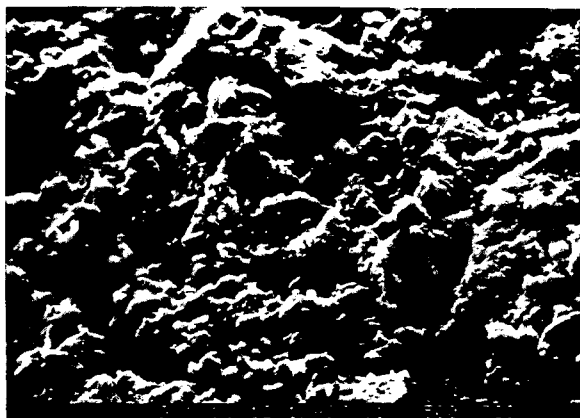


1149°C, Reducing Gas

FIGURE 4
EFFECT OF GAS ENVIRONMENT ON
AGGLOMERATION



Reducing Gas at 1149°C



Oxidizing Gas at 1149°C

FIGURE 5

ASH AGGLOMERATION USING A WESTERN SUBBITUMINOUS COAL

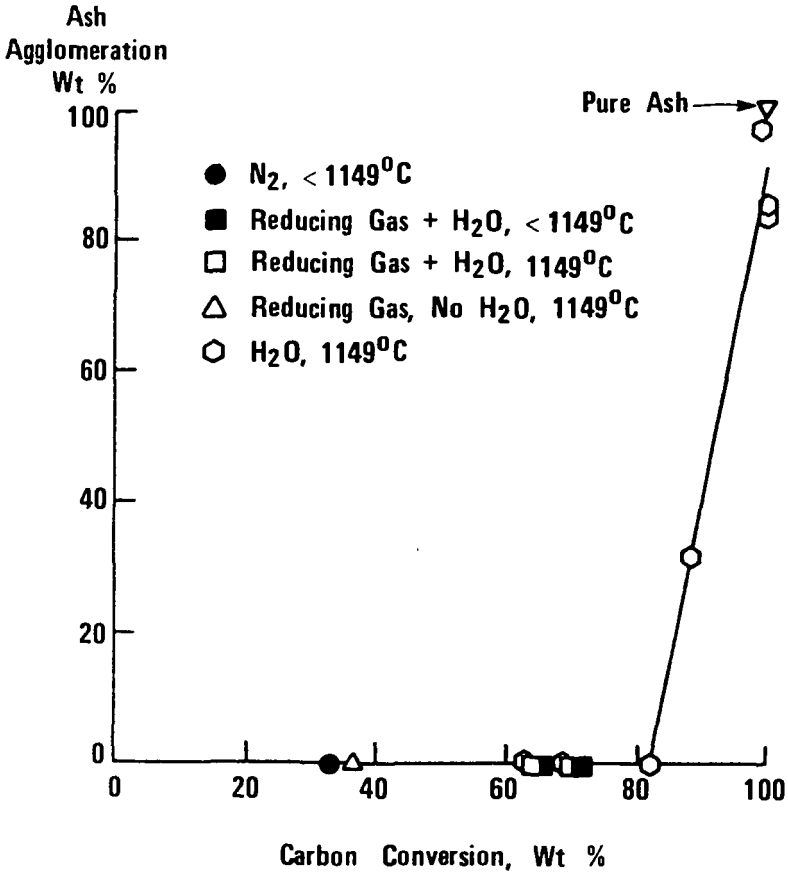
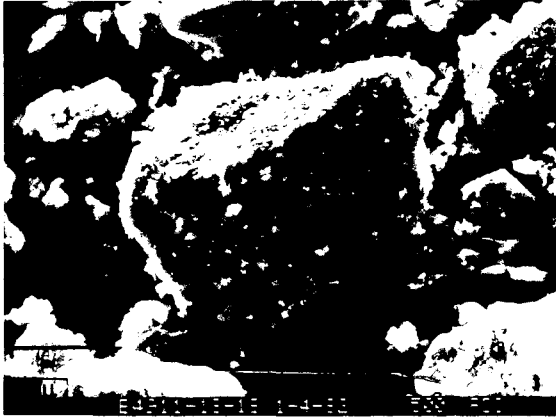


FIGURE 6
AGGLOMERATION OF
WESTERN SUBBITUMINOUS COAL NO. 2 AT 1149°C



Reducing Gas, 64 Wt % Conversion



Steam, 99 Wt % Conversion

FIGURE 7
EFFECT OF TEMPERATURE AND
INERT MATERIAL ON
ASH AGGLOMERATION IN REDUCING GAS

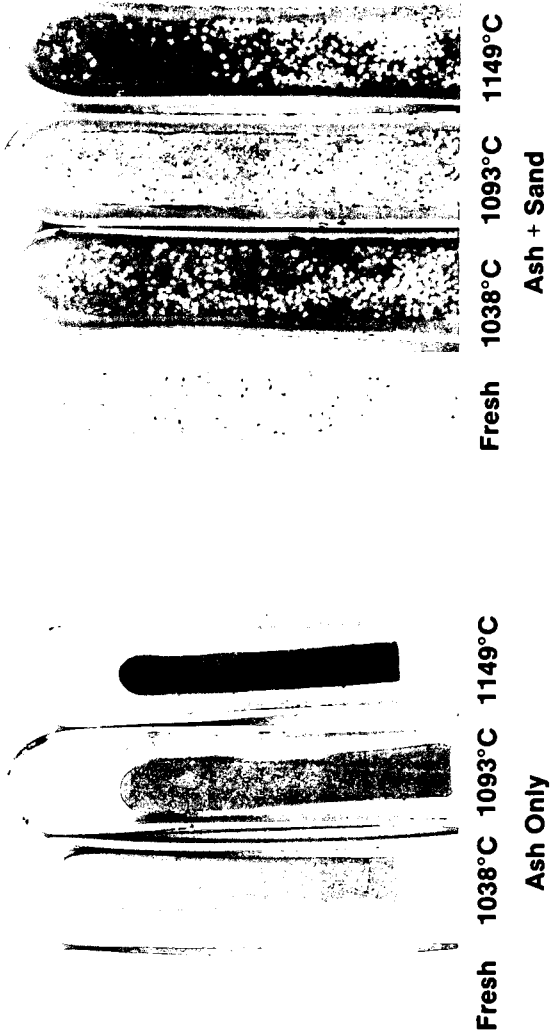


FIGURE 8
AGGLOMERATION TEMPERATURE VERSUS
INITIAL DEFORMATION TEMPERATURE

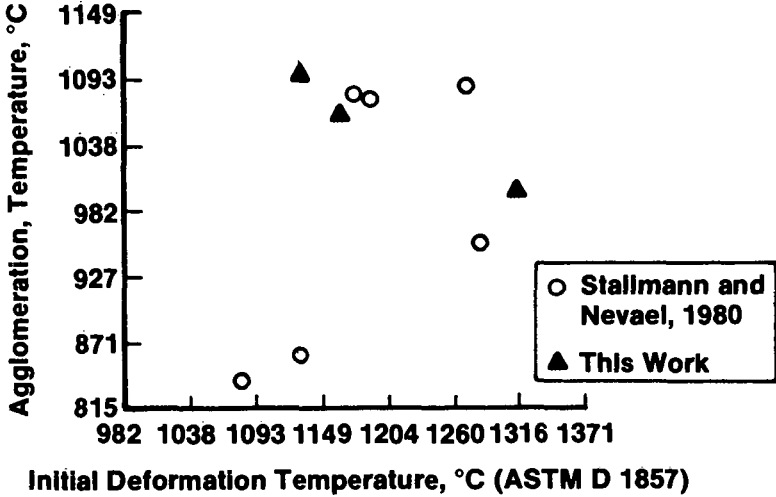


FIGURE 9
THE EFFECT OF SODIUM CONTENT ON
ASH AGGLOMERATION

